Scanning tunneling spectroscopy and topography of Si(111)-$c2\times8$ and coexisting 7×7 and 2×1 reconstructions: Surface electronic band structure

Franck Rose,[1,2,*] Shigeki Kawai,[2] Takanori Ishii,[2] and Hideki Kawakatsu[1,2,3]

[1]*Laboratory for Integrated MicroMechatronic Systems/Centre National de la Recherche Scientifique, University of Tokyo, Komaba 4-6-1, Tokyo 153-8505, Japan*

[2]*Center for International Research on Micro Mechatronics, Institute of Industrial Science, University of Tokyo, 4-6-1 Komaba, Meguro-ku, Tokyo 153-8505, Japan*

[3]*Japan Science and Technology Agency, Core Research for Evolutional Science and Technology, 4-1-8 Hon-machi, Kawaguchi, Saitama 332-0012, Japan*

(Received 17 June 2005; revised manuscript received 21 November 2005; published 11 January 2006)

The electronic band structure of the Si(111)-$c2\times8$ surface is reported by means of scanning tunneling spectroscopy. The surface is found to be semiconducting with adatom and rest atom bands lying inside the 0.8 eV energy band gap. The local density of states as well as the surface reactivity toward residual hydrogen atoms adsorption are compared for the $c2\times8$, 7×7, and 2×1 reconstructions coexisting on the same (111) quenched surface. We show that the rest atoms of the Si(111)-$c2\times8$ surface are the sites for individual hydrogen adsorption, inducing a local reverse charge transfer from the reconstruction.

DOI: 10.1103/PhysRevB.73.045309 PACS number(s): 68.35.Bs, 73.20.At, 68.37.Ef

Since the invention of the scanning tunneling microscope[1] (STM), the Si(111) surface has been the prototypical system for nanoscale investigations of surface electronic states and reconstructions. STM topography eventually revealed the topological differences between the stable Si(111)-7×7 reconstructed surface, the quenched Si(111) surface containing metastable phases[2,3] such as $2\times2m$ (2×2, $c2\times4$, and $c2\times8$), $\sqrt{3}\times\sqrt{3}$, and $2n+1\times2n+1$ (with $n>3$), and the cleavage induced Si(111)-2×1 surface.[4] Thus, the different models describing the 7×7, $c2\times8$, and 2×1 reconstructions of the Si(111) surface have been proven correct, respectively: the dimer-adatom-stacking-fault model,[5] a simple adatom rest atom model,[6,7] and the π-bonded chains model.[8] Later, the atomically resolved scanning tunneling spectroscopy technique[9] (STS) enabled the electronic surface states probing, confirming indeed that the nature of Si(111)-7×7 is metallic,[9] and that the nature of Si(111)-2×1 is semiconducting.[10]

Different reconstructions of the same surface may lead to different physical and chemical properties. In order to identify and understand these differences in the case of Si(111), a systematic experimental study of the local density of states (LDOS) of the 7×7, $c2\times8$, and 2×1 reconstructions is needed. Here, we present such a systematic comparison of the Si(111)-7×7, Si(111)-$c2\times8$, and Si(111)-2×1 reconstructions, coexisting on the very same quenched sample surface by means of room temperature (RT), STS, and STM. We show that contrary to the Ge(111)-$c2\times8$ case[7,11,12] one adatom and one rest atom bands are observed by STS in the electronic band gap of the Si(111)-$c2\times8$ surface, in good agreement with predictions by *ab initio* calculations by Bechstedt *et al.*,[13] band structure calculations by Takeuchi,[14] and STM topography by Koike *et al.*[6]

Preparation of Si(111) surfaces having simple adatom rest atom structures can only be achieved by laser[2] or thermal radiation[3,15–18] quenching from the 1×1 phase above 830 °C, possibly followed by Si deposition.[19,20] Dynamics and growth mechanism studies[16,17] of the reversible phase transition between $c2\times8$ and 1×1 structures, with a phase transition temperature[18] T_c of 230 °C, showed that the $c2\times8$ structure is the most stable of all metastable superlattices. To expose by cleavage[4,10,21–25] the (111) face of the silicon crystal results in a metastable 2×1 π-bonded chains reconstructed surface.[2] The 2×1 reconstruction is also found on molecular beam epitaxy grown,[26–30]and sputter-annealed Si(111)-7×7 surfaces,[31] and can be generated using the STM tip manipulation and surface modification methods.[32,33] Moreover, silicon π-bonded chains are likely present on the metal induced Si(111)-3×1 family of reconstructed surfaces.[34–37] Most important to the study presented here is the formation of 2×1 structures on quenched-sputtered-annealed surfaces,[38] and rapidly quenched surfaces.[39]

We used the rapid thermal radiation quenching[39] method to create 2×1 islands that coexist with the 7×7 and $c2\times8$ reconstructions. Fast sample cooling during quenching was the key to obtain 7×7, $c2\times8$, and 2×1 reconstructions coexisting on the same Si(111) surface (a cooling rate of 450 °C s^{-1} was measured with an IMPAC Infrared GmbH IGA-140 pyrometer). Samples cut from silicon wafers (1 mm$\times$7 mm$\times$0.3 mm, *n*-type, *P* doped, resistivity 0.1 Ω cm, CZ grown crystal by JEOL) were cleaned in ultrasonic baths of acetone and ethanol for 30 min, outgassed overnight in the ultrahigh vacuum (UHV) chamber (pressure $P=1.5\times10^{-8}$ Pa), and then transferred to the RT-STM stage (JSPM-4500S by JEOL). Electromigration[40]by direct current heating (5 min at 1300 °C) was used to create large flat step-free terraces. Finally reconstructed surfaces were prepared as follows: samples were raised very rapidly from RT to 900 °C, flashed for 5 s at 1320 °C, quenched from 1320 °C to RT by cutting off the heating current, annealed for 1 h at a temperature of 200 °C, and thermalized at room temperature for another hour. All STM and STS experiments presented here have been performed with several homemade metallic tips (polycrystalline W tips electrochemically pre-

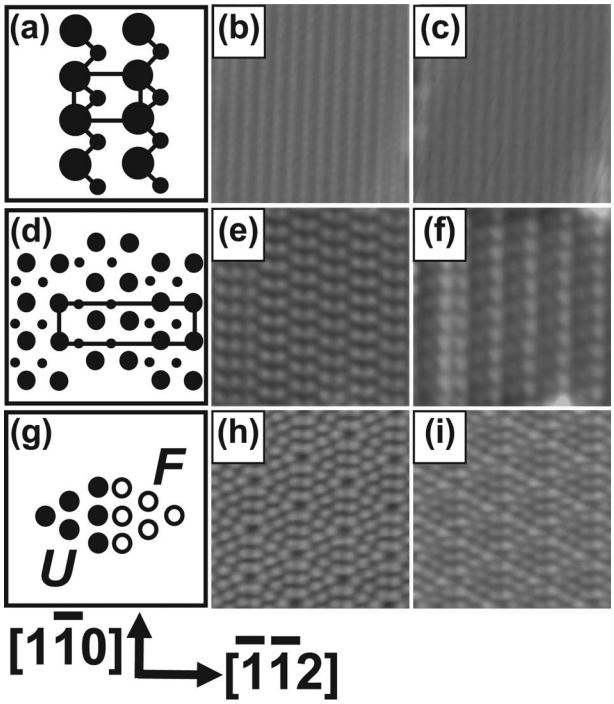

FIG. 1. Atomic diagrams [(a), (d), and (g)], and atomically resolved constant current images (100×100 Å^2) of the empty and filled electronic states of the Si(111)-2×1 [(b) and (c)], Si(111)-$c2\times8$ [(e) and (f)], and Si(111)-7×7 [(h) and (i)] reconstructions. (a) Representation of the π-bonded chains with the 2×1 unit cell drawn. Large and small filled circles stand, respectively, for "up" and "down" atoms of the "zig-zag" chains. (b) +2 V, 0.3 nA; (c) −1.5 V, 0.3 nA. (d) Adatom-rest atom (respectively, large-small filled circles) model of the $c2\times8$ reconstruction. The rectangular unit cell is drawn. (e) +1.4 V, 0.2 nA image of the adatoms. (f) −1.4 V, 0.2 nA image of the rest atoms. Due to buckling, two neighboring rest atoms in a double row appear with different contrasts. (g) Adatoms of a 7×7 unit cell: filled circles represent the unfaulted half (U), and open circles the faulted half (F). +2 V, 0.2 nA; (c) −2 V, 0.2 nA, the faulted half of the unit cell appears brighter.

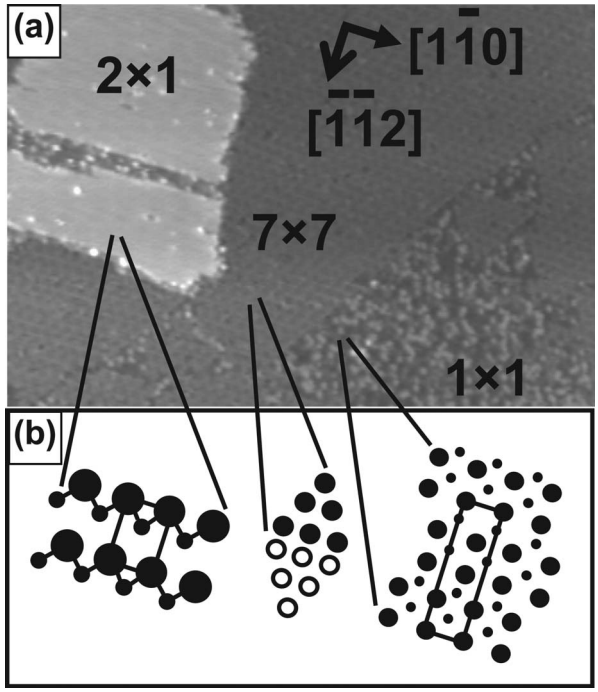

FIG. 2. Si(111)-2×1, Si(111)-7×7, and Si(111)-$c2\times8$ reconstructions, coexisting on the same quenched sample surface. (a) Constant current image (1160×760 Å^2, −2 V, 0.2 nA) showing large 2×1 islands (top left) close to a 7×7 reconstructed region, and triangular shaped metastable "1×1 areas" containing the $c2\times8$ phase. (b) From left to right: unit cells of the Si(111)-2×1, Si(111)-7×7, and Si(111)-$c2\times8$ reconstructions oriented with the proper crystallographic directions. Legends for atom representations are the same as in Fig 1.

pared in NaOH). The STM constant current mode was used for topography. All STS spectra were acquired in the sample-tip voltage range of $V=\pm2$ V, with a tunnel current set point of I=0.2 nA. For each reconstruction, the normalized conductance $(dI/dV)/|I/V|$ was numerically computed to compare with the expected LDOS.

Figure 1 displays atomically resolved STM topographs of the 7×7, $c2\times8$, and 2×1 reconstructions coexisting on the Si(111) surface area shown in Fig. 2(a). The π-bonded chains of the 2×1 reconstruction and the adatom and rest atom double rows of the $c2\times8$ reconstruction run along the $[1\bar{1}0]$ direction, while the corners of the triangles formed by "1×1 areas" and of the triangles formed by the unfaulted half of the 7×7 unit cell point in the $[11\bar{2}]$ directions. The term "1×1 area" is used here to name the triangle shaped areas (Fig. 2) containing the $2\times2m$ and $\sqrt{3}\times\sqrt{3}$ metastable phases (Fig. 5).

In Fig. 3 we present the experimentally measured LDOS spectra of the different Si(111)-7×7, Si(111)-$c2\times8$, and Si(111)-2×1 reconstructions. Thanks to our unique experimental conditions (STS performed with the same STM tip, under the same UHV and temperature conditions, and on the same sample) direct comparison is possible between these spectra. Peak positions referred to as the Fermi level E_F (V=0 V) are given in Table I and compared to existing reports from the literature. Before performing STS measurements on Si(111)-$c2\times8$ and Si(111)-2×1, we first check that our tip is metallic and good for spectroscopy by taking a Si(111)-7×7 spectrum over a corner adatom site. As expected, the Si(111)-7×7 surface [Fig. 3(c)] exhibits a metallic character with rest atom and adatom bands located, respectively, at −0.35 eV and +0.40 eV [for comparison see curve B in Fig. 5(a) of Ref. 41].

The STS spectrum measured on a "up atom" of the Si(111)-2×1 reconstruction [Fig. 3(a)] and constant current images recorded with different set points (Fig. 4) confirm that the π-bonded chains formed by the rapid radiation quenching method[39] possess the same electronic and topological properties as the π-bonded chains created by cleavage.[25] As shown in Table I, peak positions in our spectra, measured on an n-type sample, are in good overall agreement with results in the literature.[10,25,38,42] Particularly, the bands at −0.80 eV and +0.46 eV that originate, respectively, from the two states[25] πC_{CV} and πC_{CB} located at "up" and "down" atoms of the π-bonded chains are clearly resolved.

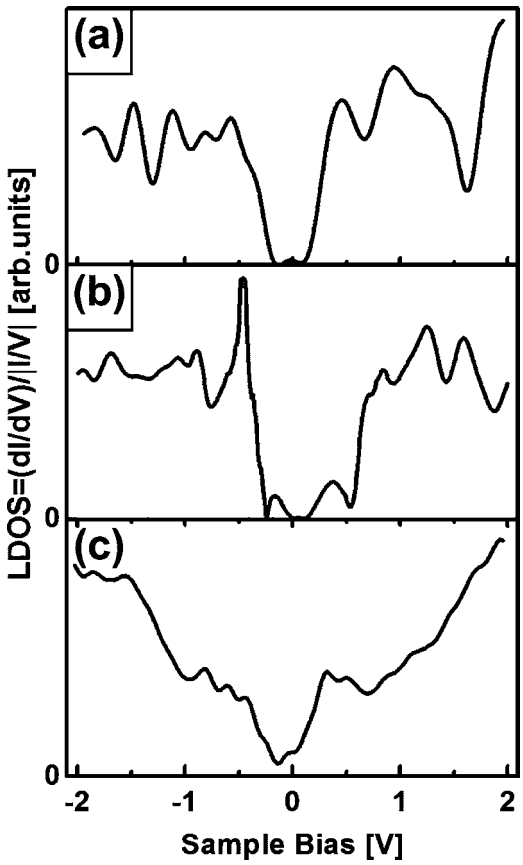

FIG. 3. Scanning tunneling spectroscopy spectra of Si(111)-2 $\times 1$, Si(111)-$c2\times 8$, and Si(111)-7×7 reconstructions coexisting on the same sample surface (sample-tip voltage range $V=\pm 2$ V, tunnel current set point I=0.2 nA). In (a), Si(111)-2×1, the tip is positioned over an up atom of a π-bonded chain [bright line in Fig. 4(a)]. In (b), Si(111)-$c2\times 8$, the tip is positioned over an adatom. The peak at −0.49 eV is artificially sharp due to difficulty in the numerical computation of the normalized conductance $(dI/dV)/|I/V|$. In (c), Si(111)-7×7, the tip is positioned over a corner hole adatom.

Within an energy shift less than 0.06 eV the peaks at −1.46, −1.1, −0.8, −0.35, +0.46, and +1.24 eV match the energy position of the peaks in Ref. 42 acquired on a *p*-type sample and of Refs. 10, 25, and 38 acquired on *n*-type samples. The fact that the results are practically independent of the doping has been already reported by Stroscio *et al.*[10] Nevertheless, we notice that in the STS spectrum of Si(111)-2×1 islands the peaks at −0.56 and +0.94 eV are shifted in energy (on the order of several 0.1 eV) when compared to the energy positions of any known peak of the cleaved Si(111)-2×1 surface spectrum. This observation could be the result of surface preparation by quenching. In comparison to the conventional preparation method by flashing for the Si(111)-7×7 surface, a considerable amount of atoms diffuses between surface steps and terraces during the quenching. Moreover *P* doping atoms might also migrate. It is thus possible that due to the small size of the islands, and due to a different organization of dopants in their vicinity, that new or shifted features appear in the band structure of the Si(111)-2×1 islands. More evidence for the π-bonded chains nature of the 2×1 tagged area of Fig. 2(a) is given by the expected topographical changes[25] in the zoomed images of Fig. 4: we observe the presence of lines running in the $[1\bar{1}0]$ direction for bias voltages outside the semiconducting band gap, and a strong emerging corrugation in both the $[1\bar{1}0]$ and $[\bar{1}\bar{1}2]$ directions for lower voltages. For comparison, our topographs were recorded with exactly the same bias voltages and tunnel currents as the ones displayed in Garleff *et al.*[25] (see Fig. 2 of Ref. 25, showing π-bonded chains created by cleavage).

The origin, formation, and geometrical structure of the Si(111)-$c2\times 8$ surface have already been investigated in detail by other groups.[2,3,15–18] In order to complete these works, we focus here on experimental results concerning the electronic behavior and chemical properties of this metastable surface phase. We present an experimentally measured STS spectrum of the Si(111)-$c2\times 8$, and discuss the arising differences in the LDOS and surface reactivity between Si(111)-$c2\times 8$ and Si(111)-7×7. The Si(111)-$c2\times 8$ STS spectrum in Fig. 3(b), taken on top of an adatom, contains features on both the empty and filled states sides and a region of low conductivity centered at +0.12 eV. The peak positions are determined by the location of the maxima in the spectrum, and uncertainty of the peak positions is estimated to be ±0.025 eV, except for the peak at −0.49 ev (±0.05 eV, see the caption of Fig. 3). A close examination of the spectrum reveals the presence of two rest atom bands, two adatom bands, and an apparent semiconducting energy band gap of 0.8 eV associated with the region of low conductivity. One rest atom band and one adatom band are located in the band gap, respectively, at −0.15 eV and +0.44 eV. The other bands are located near the valence band edge at −0.49 eV for the rest atoms, and at the conduction band edge at +0.66 eV for the adatoms. These results are in good agreement with band structures derived by *ab initio* calculations,[13] and point out the differences between the surface band structures of Si(111)-$c2\times 8$ and Ge(111)-$c2\times 8$. In the Si(111)-$c2\times 8$ band structure of Ref. 13, the dangling bonds of the two adatoms and the two rest atoms are located in the fundamental gap region and exhibit a small dispersion in the $\Gamma YY'\Gamma'$ high-symmetry direction of the two-dimensional Brillouin zone. When comparing the *p* and *s* character of the dangling bonds for diamond, silicon, and germanium, Bechstedt *et al.*[13] found that the adatom dangling bonds of silicon become more p_z-like than in carbon, and that the rest atom dangling bonds become more and more *s*-like along the group IV column C→Si→Ge. Consequently, the surface bands associated with the rest atoms are lowered in energy along the group IV column C→Si→Ge. In the Ge(111) case, tunneling spectroscopy measurements[11,12] have reported that adatom and rest atom bands are only seen outside of the band gap, respectively, deep in the valence band, and at the conduction band edge. As discussed by Bechstedt *et al.*,[13] this behavior explains the stabilization of the Ge(111) surface by the $c2\times 8$ reconstruction. In the case of Si(111)-$c2\times 8$, we indeed observed rest atom bands close to valence band edge maximum. The splitting of the rest atom band has been predicted on the basis on STM topography,[6] showing a small buckling between the two inequivalent[43] neighboring rest atoms forming $c2\times 8$ double rows. This buckling is observed

TABLE I. Peak positions column: peak positions measured in eV in the spectra of Fig. 2 (referred to as the Fermi level E_F $V=0$ V). Our results are in good overall agreement with previous reports from the literature (see text for discussions). Previous reports column: peak positions in eV noted from previous reports. In the case of the spectroscopy of the Si(111)-2×1 π-bonded chains, results are sorted by doping types. Reference 10: n-type 5 Ω cm. Reference 25: n-type, doped with 6×10^8 P atoms per cm^3. Reference 38: n-type, As doped, 0.005 Ω cm. Reference 42: p-type, 1 Ω cm. In the Si(111)-$c2\times8$ case, our measurements match the bands structure calculations by Bechstedt *et al.* (Ref. 13).

Surface reconstruction	Peak position	Previous reports	
Si(111)-7×7	−0.35	−0.35 (Ref. 41)	
	+0.40	+0.40 (Ref. 41)	
Si(111)-$c2\times8$	−0.49		
	−0.15		
	+0.44		
	+0.66		
Si(111)-2×1		p type	n type
	−1.46		−1.4 (Refs. 25 and 38)
	−1.1	−1.08 (Ref. 42)	−1.1 (Ref. 10),
	−0.8		−0.76 (Ref. 25)
	−0.56, −0.35	−0.34 (Ref. 42)	−0.4 (Ref. 38), −0.3 (Ref. 10)
	+0.46		+0.42 (Ref. 25), +0.4 (Ref. 38)
	+0.94, +1.24	+1.22 (Ref. 42)	+1.3 (Ref. 25), +1.2 (Refs. 38 and 10)

in Fig. 1(f), where the rest atom on the right-hand side of the double row running in the $[1\bar{1}0]$ direction appears higher than its neighbor (brighter in the STM topography, a difference of 0.2 Å is measured). Splitting of the adatom band is observed in the Si(111)-$c2\times8$ STS spectrum and has been previously reported in the case of Ge(111)-$c2\times8$.[11] Our description of the Si(111)-$c2\times8$ band structure from the experimental STS spectrum of Fig. 3(b) clearly shows that it is markedly different from one of the corresponding Ge(111)-$c2\times8$ surface, demonstrating that the energies of the surface bands depend strongly on the distances between surface atoms.

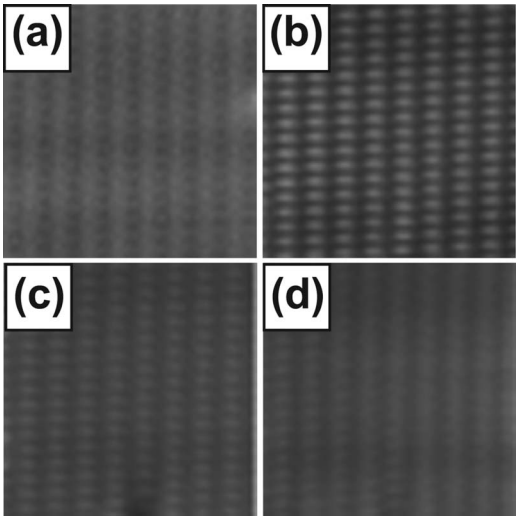

FIG. 4. Variation of the 2×1 π-bonded chains topography with different tunneling set points (120×120 Å^2; crystallographic directions are the same as displayed in Fig. 1). (a) +1.4 V, 0.5 nA; (b) +0.6 V, 0.5 nA; (c) −0.3 V, 0.1 nA; (d) −1.1 V, 0.2 nA.

It can be noted that the density of states, in the energetic region of the spectra corresponding to the adatom bands [Figs. 3(b) and 3(c)], is higher for Si(111)-7×7 than for Si(111)-$c2\times8$. This is also observed in the constant current topographies: 7×7 and $c2\times8$ regions exhibit the same corrugation at a sample bias of $V=+1.1$ V [Fig. 5(a)], but at a lower bias of $V=+0.6$ V [Fig. 5(b)] $c2\times8$ areas appear as dark depressions close to bright 7×7 areas.[16] Moreover, noncontact atomic force microscopy and scanning kelvin probe force microscopy studies[44] have reported surface potential differences between the 7×7-reconstructed and 1×1-disordered structures of the quenched Si(111) surface. All these observations suggest that Si(111)-7×7 and Si(111)-$c2\times8$ reconstructions have a different work function,[45] which could locally induce on the same sample surface very different chemical reactivity toward atomic or molecular adsorption.

An examination of large scale areas of surfaces being studied for a few hours in the STM chamber revealed the appearance of features on the Si(111)-$c2\times8$ reconstruction (Fig. 6), comparable to the "triangle" and "square" sites[12,46] observed after adsorption of hydrogen atoms on the Ge(111)-$c2\times8$ surface. Hydrogen atoms are believed to be formed from the residual gas of the UHV chamber, containing H_2 molecules dissociated by the ion gauge filament. In

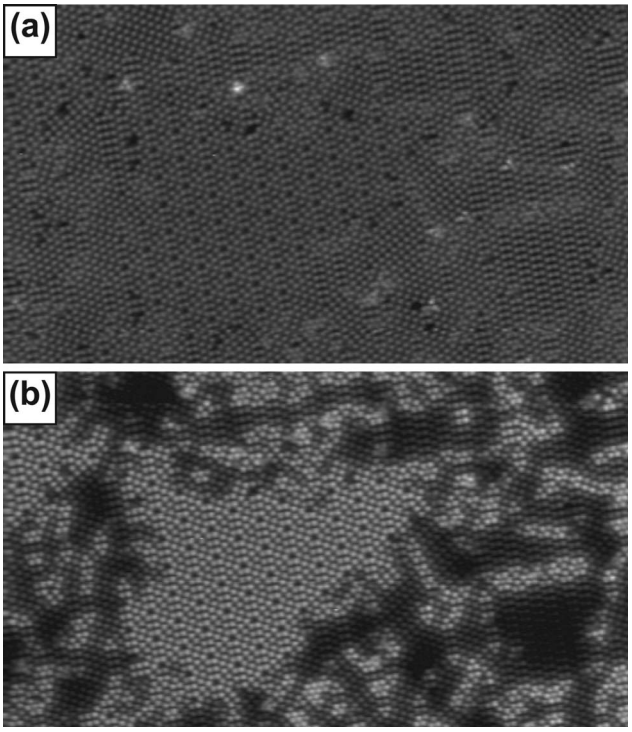

FIG. 5. Differences in the contrast behavior of constant current topographies of the filled states of Si(111)-7×7 and Si(111)-$c2\times8$ (650×370 Å^2). (a) +1.1 V, 0.2 nA; (b) +0.6 V, 0.2 nA. Due to a lower LDOS in the adatoms bands energetic region, the $c2\times8$ areas become darker than the 7×7 areas. It is note that $2\times2m$ and $\sqrt{3}\times\sqrt{3}$ metastable phases are also observed here.

the topography of the filled states [Fig. 6(b)], we observe a dark depression at the rest atom site, and four bright protrusions at the closest neighboring adatom sites. By comparison with the Ge(111)-$c2\times8$ case,[12,46] we interpret the image of the "square" feature in Fig. 6 with the adsorption of a single hydrogen atom on top of a rest atom site, inducing a reverse charge transfer from the $c2\times8$ reconstruction. After 16.5 h in the UHV chamber, we measured a very small coverage of these features on the Si(111)-$c2\times8$ reconstruction, and when the gauge filament was turned off no feature appeared. No adsorption has been observed on the coexisting Si(111)-7×7 and Si(111)-2×1 reconstructions for the same residual gas exposure and the same observed size area. This suggests that $c2\times8$ ar-eas are more reactive toward hydrogen adsorption than the two other kinds of reconstructed regions. We calculate the sticking coefficient by the following equation: $\eta=(N/N_0)(2\pi mkT)^{1/2}/(\mathrm{Pt}S_0)$, where N/N_0 is the ratio of reacted sites over nonreacted sites, m is the hydrogen atom mass, k the Boltzmann's constant, T the temperature, P the pressure during exposure, t the time of exposure, and S_0 the surface area of the site. We find $\eta_{c2\times8}=2\times10^{-3}$ for the Si(111)-$c2\times8$ surface, and estimate $\eta_{7\times7}=3\times10^{-4}$ for the Si(111)-7×7 surface from the results reported in Ref. 47, confirming our experimental observations. In conclusion, we have observed that the $c2\times8$ reconstruction of the Si(111) surface has the same behavior than the one of the Ge(111)surfaces toward H atoms adsorption, which suggests that the influence of the reconstruction dominates the reactivity rather than the chemical nature of the surface. Compared to a previous report[48] on Ge(111)-$c2\times8$, experiments concerning the adsorption of molecular oxygen on the Si(111)-$c2\times8$ surface also confirm this concluding remark and will be the subject of another communication.[49]

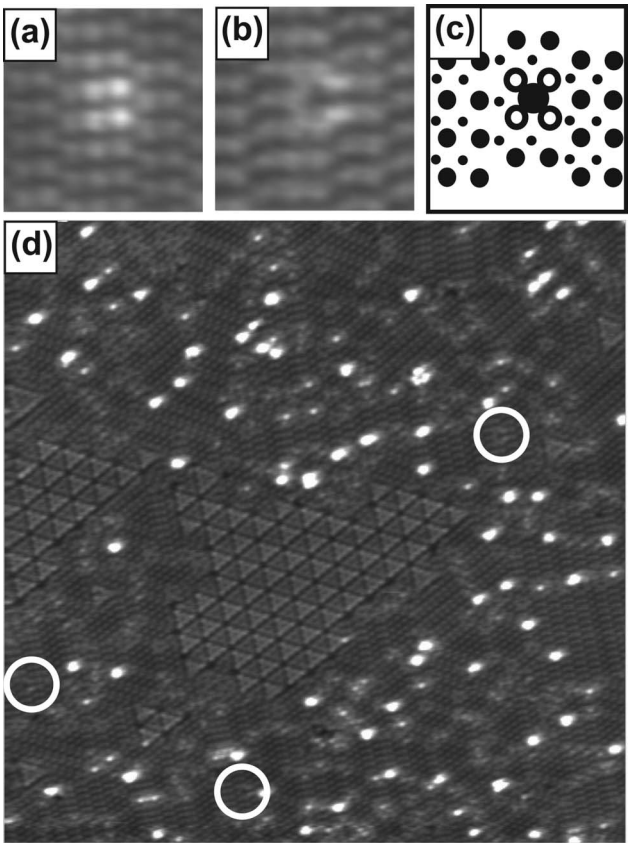

FIG. 6. (a) and (b) Residual hydrogen atom adsorbed on a "square" rest atom site [54×54 Å^2, circled area in the top right corner of (d)]. (a) Constant current image of the adatoms (empty electronic states, +0.6 V, 0.2 nA). (b) Hydrogen adsorption is accompanied with a reverse charge transfer from the reconstruction: the rest atom adsorption site becomes dark, and the four surrounding adatoms become bright in the constant current image of the filled electronic states (−2 V, 0.2 nA). (c) Atomic diagram of a "square site:" larger, middle, and small filled circles represent, respectively, the hydrogen atom adsorbed on a rest atom site, the adatoms, and the rest atoms. The open circles stand for the four bright adatoms in the constant current image of the filled electronic states. (d) Filled electronic states image (−2 V, 0.2 nA) of the surface area displayed in Fig. 5 (larger size 650×650 Å^2), the three white circles mark square sites. This hydrogen coverage corresponds to 16.5 h exposure of residual gas ($P=1.5\times10^{-8}$ Pa).

In summary, using the rapid thermal radiation quenching method,[39] we were able to prepare Si(111)-7×7, Si(111)-$c2\times8$, and Si(111)-2×1 reconstructions, coexisting on the same sample surface. STM topography and spectroscopy showed that the 2×1 π-bonded chains created by this method are of the same electronic and topological nature as the chains created by cleavage. LDOS of the Si(111)-$c2\times8$ reconstruction obtained by STS shows, as predicted by calculations[13] dealing with the origin of the different reconstructions of group IV semiconductor surfaces, that contrary

to the stabilized Ge(111)-$c2\times8$ surface, the metastable Si(111)-$c2\times8$ surface exhibits adatom and rest atoms surface bands inside the energy band gap, respectively, at +0.44 and −0.15 eV. We measured an 0.8 eV wide energy band gap, and attribute a semiconducting character to the Si(111)-$c2\times8$ surface reconstruction. Similarly to the Ge(111)-$c2\times8$ surface, the rest atom sites of the Si(111)-$c2\times8$ surface have been found to be the sites for residual hydrogen atom adsorption, inducing a local reverse charge transfer from the rest atom to the adatom. We finally draw the conclusions that in the case of group IV semiconductors, first, the nature of the atoms and the distance between them change radically the surface band structure for the same reconstruction; second, the reconstruction seems to be the most influent parameter when comparing the chemical reactivity of surfaces of different atomic nature.

This work has been financially supported by JST-CREST and the JSPS.

*Corresponding author. Email address: frose@iis.u-tokyo.ac.jp

[1] G. Binnig, H. Rohrer, Ch. Gerber, and E. Weibel, Phys. Rev. Lett. **50**, 120 (1983).
[2] R. S. Becker, J. A. Golovchenko, G. S. Higashi, and B. S. Swartzentruber, Phys. Rev. Lett. **57**, 1020 (1986).
[3] T. Hoshino, K. Kokubun, K. Kumamoto, T. Ishimaru, and I. Odhomari, Jpn. J. Appl. Phys., Part 1 **34**, 3346 (1995).
[4] R. M. Feenstra, W. A. Thompson, and A. P. Fein, Phys. Rev. Lett. **56**, 608 (1986).
[5] K. Takayanagi, Y. Tanishiro, M. Takahashi, and S. Takahashi, J. Vac. Sci. Technol. A **3**, 1502 (1985); K. Takayanagi, Y. Tanishiro, M. Takahashi, and S. Takahashi, Surf. Sci. **164**, 367 (1985).
[6] M. Koike, Y. Einaga, H. Hirayama, and K. Takayanagi, Phys. Rev. B **55**, 15444 (1997).
[7] R. S. Becker, B. S. Swartzentruber, J. S. Vickers, and T. Kilstner, Phys. Rev. B **39**, 1633 (1989).
[8] K. C. Pandey, Phys. Rev. Lett. **47**, 1913 (1981); K. C. Pandey, Phys. Rev. Lett. **49**, 223 (1982).
[9] R. J. Hamers, R. M. Tromp, and J. E. Demuth, Phys. Rev. Lett. **56**, 1972 (1986).
[10] J. A. Stroscio, R. M. Feenstra, and A. P. Fein, Phys. Rev. Lett. **57**, 2579 (1986).
[11] R. M. Feenstra, G. Meyer, and K. H. Rieder, Phys. Rev. B **69**, 081309(R) (2004); R. M. Feenstra, S. Gaan, G. Meyer, and K. H. Rieder, *ibid.* **71**, 125316 (2005).
[12] G. Dujardin, A. J. Mayne, and F. Rose, Phys. Rev. Lett. **89**, 036802 (2002).
[13] F. Bechstedt, A. A. Stekolnikov, J. Furthmüller, and P. Käckell, Phys. Rev. Lett. **87**, 016103 (2001).
[14] N. Takeuchi, Phys. Rev. B **57**, 6255 (1998).
[15] Y. -N. Yang and E. D. Williams, Phys. Rev. Lett. **72**, 1862 (1994).
[16] M. Chida, Y. Tanishiro, H. Minoda, and K. Yagi, Surf. Sci. **441**, 179 (1999).
[17] M. Chida, Y. Tanishiro, H. Minoda, and K. Yagi, Surf. Sci. **423**, L236 (1999).
[18] M. Chida, H. Minoda, Y. Tanishiro, and K. Yagi, Surf. Sci. **411**, L822 (1998).
[19] Z. Zhang, M. A. Kulakov, and B. Bullmer, Surf. Sci. **375**, 195 (1997).
[20] H. Minoda, T. Sato, K. Yagi, Y. Tanishiro, and M. Iwatsuki, Surf. Sci. **493**, 157 (2001).
[21] J. J. Lander, F. Gobeli, and J. Morrison, J. Appl. Phys. **34**, 2298 (1963).
[22] R. M. Feenstra, W. A. Thompson, and A. P. Fein, J. Vac. Sci. Technol. A **4**, 1315 (1986).
[23] J. A. Stroscio, R. M. Feenstra, and A. P. Fein, J. Vac. Sci. Technol. A **5**, 838 (1987).
[24] R. M. Feenstra and M. A. Lutz, Surf. Sci. **243**, 151 (1991).
[25] J. K. Garleff, M. Wenderoth, K. Sauthoff, R. G. Ulbrich, and M. Rohfing, Phys. Rev. B **70**, 245424 (2004).
[26] C. J. Lanczycki, R. Kotlyar, E. Fu, Y. -N. Yang, E. D. Williams, and S. Das Sarma, Phys. Rev. B **57**, 13132 (1998).
[27] T. Fukuda, Phys. Rev. B **59**, 9752 (1999).
[28] T. Yokoyama, H. Tanaka, M. Itoh, T. Yokotsuka, and I. Sumita, Phys. Rev. B **49**, 5703 (1994).
[29] Y. Shigeta, J. Endo, and K. Maki, Phys. Rev. B **51**, R2021 (1995).
[30] Y. -N. Yang and E. D. Williams, Phys. Rev. B **51**, 13238 (1995).
[31] M. D. Pashley, K. W. Haberern, and W. Friday, J. Vac. Sci. Technol. A **6**, 488 (1988).
[32] R. S. Becker, G. S. Higashi, Y. J. Chabal, and A. J. Becker, Phys. Rev. Lett. **65**, 1917 (1990).
[33] J. I. Pascual, C. Rogero, J. Gómez-Herrero, and A. M. Baró, Phys. Rev. B **59**, 9768 (1999).
[34] A. A. Saranin, A. V. Zotov, V. G. Lifshits, M. Katayama, and K. Oura, Surf. Sci. **426**, 298 (1999).
[35] T. Okuda, H. Shigeoka, H. Daimon, S. Suga, T. Kinoshita, and A. Kakizaki, Surf. Sci. **321**, 105 (1994).
[36] T. Okuda, K. Sakamoto, H. Nishimoto, H. Daimon, S. Suga, T. Kinoshita, and A. Kakizaki, Phys. Rev. B **55**, 6762 (1997).
[37] K. Sakamoto, T. Okuda, H. Nishimoto, H. Daimon, S. Suga, T. Kinoshita, and A. Kakizaki, Phys. Rev. B **50**, 1725 (1994).
[38] R. S. Becker, T. Kilstner, and J. S. Vickers, Phys. Rev. B **38**, 3537 (1988).
[39] M. A. Kulakov, Surf. Sci. **372**, L266 (1997).
[40] A. V. Latyshev, A. L. Aseev, A. B. Krasilnikov, and S. I. Stenin, Surf. Sci. **213**, 157 (1989).
[41] Ph. Avouris and R. Wolkow, Phys. Rev. B **39**, 5091 (1989).
[42] R. M. Feenstra, Phys. Rev. B **44**, R13791 (1991).
[43] Two neighboring rest atoms (adatoms) are inequivalent because one of them is surrounded by three adatoms (rest atoms), while the other one by four adatoms (rest atoms).
[44] T. Shiota and K. Nakayama, Jpn. J. Appl. Phys., Part 1 **40**, L986 (2001).
[45] W. Mönch, in *Semiconductor Surfaces and Interfaces*, edited by G. Ertl, H. Lüth, and D. L. Mills, Springer Series in Surface Sciences Vol. 26 (Springer, Berlin, 1995).

[46] G. Dujardin, F. Rose, and A. J. Mayne, Phys. Rev. B **63**, 235414 (2001).
[47] K. Mortensen, D. M. Chen, P. J. Bedrossian, J. A. Golovchenko, and F. Besenbacher, Phys. Rev. B **43**, 1816 (1991).
[48] A. J. Mayne, F. Rose, and G. Dujardin, Surf. Sci. **523**, 157 (2003).
[49] F. Rose, S. Kawai, and H. Kawakatsu, Surf. Sci. (to be published).